J Digit Imaging (2015) 28:213–223
DOI 10.1007/s10278-014-9725-9

Classification of Hypervascular Liver Lesions Based on Hepatic Artery and Portal Vein Blood Supply Coefficients Calculated from Triphasic CT Scans

F. Edward Boas · Aya Kamaya · Bao Do · Terry S. Desser · Christopher F. Beaulieu · Shreyas S. Vasanawala · Gloria L. Hwang · Daniel Y. Sze

Published online: 3 September 2014

Abstract Perfusion CT of the liver typically involves scanning the liver at least 20 times, resulting in a large radiation dose. We developed and validated a simplified model of tumor blood supply that can be applied to standard triphasic scans and evaluated whether this can be used to distinguish benign and malignant liver lesions. Triphasic CTs of 46 malignant and 32 benign liver lesions were analyzed. For each phase, regions of interest were drawn in the arterially enhancing portion of each lesion, as well as the background liver, aorta, and portal vein. Hepatic artery and portal vein blood supply coefficients for each lesion were then calculated by expressing the enhancement curve of the lesion as a linear combination of the enhancement curves of the aorta and portal vein. Hepatocellular carcinoma (HCC) and hypervascular metastases, on average, both had increased hepatic artery coefficients compared to the background liver. Compared to HCC, benign lesions, on average, had either a greater hepatic artery coefficient (hemangioma) or a greater portal vein coefficient (focal nodular hyperplasia or transient hepatic attenuation difference). Hypervascularity with washout is a key diagnostic criterion for HCC, but it had a sensitivity of 72 % and specificity of 81 % for diagnosing malignancy in our diverse set of liver lesions. The sensitivity for malignancy was increased to 89 % by including enhancing lesions that were hypodense on all phases. The specificity for malignancy was increased to 97 % (p=0.039) by also examining hepatic artery and portal vein blood supply coefficients, while maintaining a sensitivity of 76 %.

Keywords Triphasic CT · Enhancement · Washout · Hepatocellular carcinoma · Liver lesions · Computer-aided diagnosis

Abbreviations

AASLD	American Association for the Study of Liver Diseases
EASL	European Association for the Study of the Liver
FNH	Focal nodular hyperplasia
HAC	Hepatic artery coefficient or hepatic artery blood supply coefficient
HCC	Hepatocellular carcinoma
HU	Hounsfield units
PVC	Portal vein coefficient or portal vein blood supply coefficient
RFA	Radiofrequency ablation
ROI	Region of interest
TACE	Transarterial chemoembolization
THAD	Transient hepatic attenuation difference

F. E. Boas (✉)
Interventional Radiology, Memorial Sloan Kettering Cancer Center, 1275 York Ave, New York, NY 10065, USA
e-mail: boas@post.harvard.edu

A. Kamaya · T. S. Desser · C. F. Beaulieu · S. S. Vasanawala · G. L. Hwang · D. Y. Sze
Department of Radiology, Stanford University Medical Center, Stanford, CA 94305, USA

B. Do
VA Palo Alto Health Care System, Palo Alto, CA 94304, USA

Introduction

A variety of benign and malignant liver lesions can be characterized using contrast-enhanced CT. The optimal times for imaging the liver are during the late-arterial phase (35 s after contrast injection), when hypervascular liver lesions tend to have the greatest enhancement relative to background liver, the portal venous phase (60–70 s), when hypovascular liver metastases and the portal veins are best visualized, and the

delayed (or equilibrium) phase (3–5 minutes), when washout or contrast retention can be best characterized. The non-enhanced phase provides minimal additional diagnostic information for liver lesions [1, 2], and to reduce the radiation dose, it is no longer part of our institution's multiphasic liver CT protocol.

On triphasic CT, hepatocellular carcinoma (HCC) is characteristically hyperdense compared to the surrounding liver in the arterial phase, isodense or hypodense compared to the liver in the portal venous phase, and hypodense compared to the liver in the delayed phase [1, 3]. Arterial phase enhancement (hyperdense compared to surrounding liver) with portal venous or delayed phase washout of contrast (hypodense compared to surrounding liver) [4] is considered diagnostic of HCC in cirrhotic livers, according to both European Association for the Study of the Liver (EASL) [5] and American Association for the Study of Liver Diseases (AASLD) [6] guidelines.

However, not all HCCs demonstrate contrast washout on delayed imaging, and not all lesions with washout are HCCs. A minority of well-differentiated HCCs are hypodense to the liver on all phases [7]. Some hypervascular HCCs do not have washout [8]. Washout can also be seen in other liver lesions (both benign and malignant), including regenerative nodules [9], hemangiomas [10], focal nodular hyperplasia (FNH) [11], adenomas [12], and hypervascular metastases such as neuroendocrine tumors [13].

The appearance of the liver on various phases of imaging is thought to be related to the liver's dual blood supply. The normal liver receives about 70 % of its blood flow from the portal vein and 30 % from the hepatic artery [14]. HCC receives most of its blood flow from the hepatic artery [15], which enhances and de-enhances before the portal vein does. Washout is presumably related to rapid displacement of highly enhanced blood with less enhanced blood in tissue that is predominantly supplied by the hepatic artery.

Liver perfusion CT typically involves scanning the liver at numerous (>20) time points after injection of IV contrast. The resulting enhancement curves can then be used to calculate blood volumes, blood flow, and capillary permeability [15, 16]. One goal of perfusion CT is to improve detection and characterization of liver lesions compared to standard triphasic imaging [16]. However, perfusion CT typically requires dedicated protocols and a large radiation dose, and the role of perfusion parameters in distinguishing benign and malignant liver lesions has not yet been established.

To address these limitations, we introduce the concept of the hepatic artery and portal vein blood supply coefficients (HAC and PVC), which provide a simple way to characterize enhancement curves quantitatively on standard triphasic CTs (arterial, portal venous, and delayed phases). We propose using the HAC and PVC to classify hypervascular liver lesions and to increase diagnostic accuracy by computer-aided diagnosis.

The HAC and PVC describe the enhancement curve of a liver lesion (which only contain 3 points in a triphasic scan) as a linear combination of the aortic and portal venous enhancement curves (Fig. 1). For example, an enhancement curve that has the same shape as the aortic enhancement curve, but only half the amount of enhancement, is considered to have 50 % HAC. An enhancement curve that is halfway between the enhancement curves of the aorta and portal vein is considered to have 50 % HAC and 50 % PVC. Thus, HAC indicates similarity of a lesion's enhancement curve to the aortic enhancement curve, and PVC indicates similarity of a lesion's enhancement curve to the portal venous enhancement curve.

The HAC and PVC are equal to hepatic artery and portal vein blood volumes, in a simple perfusion model that assumes rapid blood flow (no delay between enhancement of the supplying vessel and the tissue) and no vascular permeability to contrast (Fig. 2). Blood volumes or coefficients are

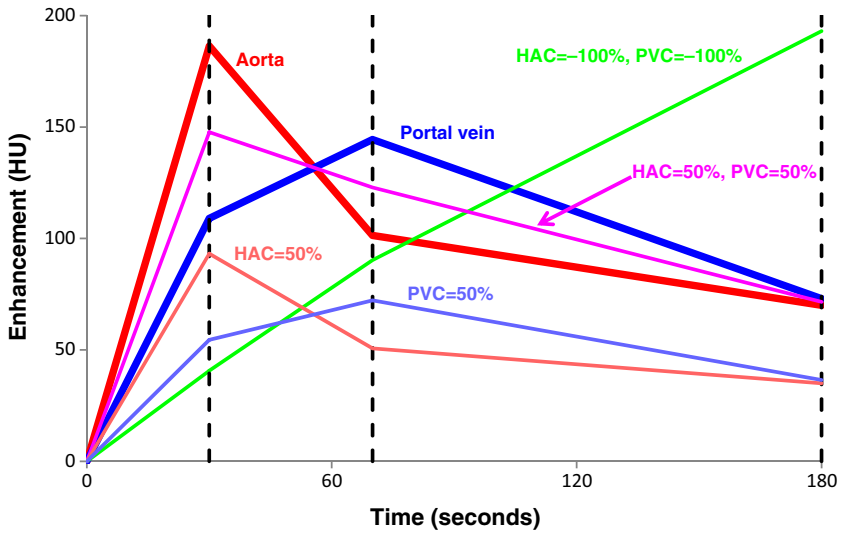

Fig. 1 Schematic diagram of hepatic artery and portal vein coefficients calculated from a triphasic CT. The enhancement curve of a tumor or surrounding liver is expressed as a linear combination of the aortic and portal venous enhancement curves. The three phases in the triphasic scan are indicated by *vertical dashed lines*. The measured enhancement curves of the aorta and portal vein are plotted using *thick lines*. Other enhancement curves (*thin lines*) are labeled with their calculated coefficients

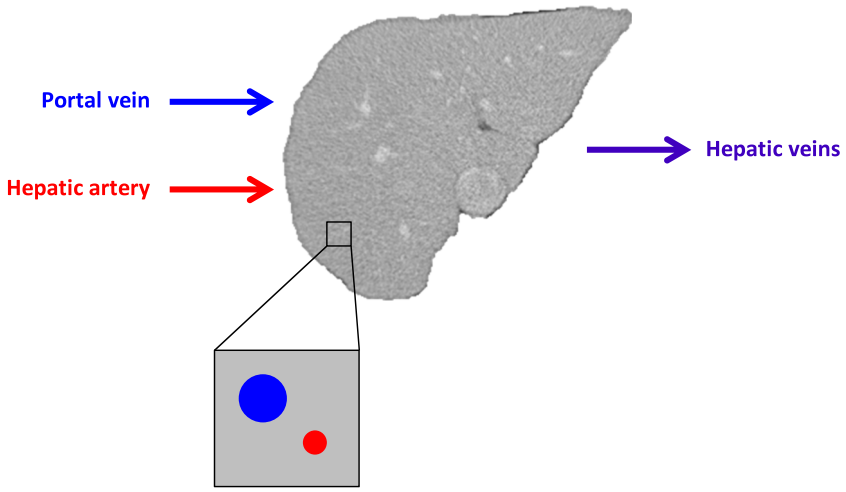

Fig. 2 Simple model of liver perfusion. Branches of the portal vein are assumed to have the same enhancement curve as the main portal vein. Branches of the hepatic artery are assumed to have the same enhancement curve as the aorta. The enhancement of the liver parenchyma is due to small vessels that are below the resolution of CT. Normal liver parenchyma contains both portal vein and hepatic artery branches, so the enhancement will be a linear combination of the portal vein and hepatic artery enhancement curves. A hypervascular tumor will contain a greater proportion of hepatic artery branches, and the enhancement curve will more closely follow the hepatic artery enhancement curve

expressed in units of blood volume in a voxel (ml) divided by total volume of the voxel (ml) or as a percentage. Lesions with high HAC will show washout, compared to the background liver, which has high PVC. Delayed enhancement (green line in Fig. 1) cannot be explained by a model that assumes rapid flow and no leakage of contrast from vessels. However, since the enhancement increases in the delayed phase, whereas both the aorta and portal vein have decreased enhancement in the delayed phase, the green line has a negative calculated HAC and PVC. In the case of delayed enhancement, the calculated HAC and PVC describe the shape of the enhancement curve but do not correspond to actual blood volumes.

In this paper, we examine whether HAC and PVC calculated from standard triphasic CTs can be used to distinguish benign and malignant liver lesions.

Materials and Methods

Patient Selection and Scan Parameters

The institutional review board approved this retrospective HIPAA compliant study; informed patient consent was waived. A diverse set of liver lesions with pretreatment triphasic CT scans was obtained by searching for diagnoses that can be hypervascular. A database of radiology reports (impression section only) was searched for the following terms: focal nodular hyperplasia, transient hepatic attenuation difference, arterioportal shunt, adenoma, hypervascular metastasis, hemangioma, and regenerative nodule. In addition, a database search was performed to identify HCCs that were treated by resection, transplant, transarterial chemoembolization (TACE), or radiofrequency ablation (RFA). The two largest lesions on the pretreatment scan were examined.

Typical scan parameters were as follows: 120–150 ml of iodinated contrast (iopamidol 300–370 mg iodine/ml) was power injected intravenously at a rate of 4–5 ml/s. The liver was imaged at 30–35 s (arterial phase), 60–70 s (portal venous phase), and 180 s (delayed phase) after the start of contrast injection, using a kVp of 100–120 [4]. The following scanners were used: Siemens Definition, Siemens Definition AS+, Siemens SOMATOM Definition, Siemens Sensation 64, GE Discovery CT750 HD, GE LightSpeed 16, and GE LightSpeed VCT. Images were reconstructed using a soft tissue kernel, with a slice thickness between 1 and 5 mm.

For each diagnosis, cases with pretreatment triphasic CT scans were evaluated for inclusion in the study (Table 1). Cases were excluded if the arterially enhancing portion of the lesion was too small to characterize (≤5 mm) or if the main portal vein was completely occluded. In addition, cases were excluded if the peak enhancement of the aorta was not during the arterial phase or the peak enhancement of the portal vein was not during the portal venous phase. This eliminated cases where the aorta and portal vein had similar enhancement curves (due to a poor bolus or mis-timed scan), which would make it difficult to calculate accurate coefficients.

The diagnosis was based on the radiology reports (including MRI and follow-up studies) and pathology (if available). Many of the lesions did not have pathologic confirmation. This allowed us to analyze lesions with classic imaging features that are not biopsied, as well as borderline lesions that are followed by imaging, but never biopsied. Regenerative nodules that did not have pathologic confirmation had to meet all of the following criteria: resolution on follow-up imaging or stability for at least 250 days, normal AFP, and no suspicious

Table 1 Liver lesions examined in this study

Diagnosis	Initial number of lesions	Number of excluded lesions	Final number of lesions	Pathology proven (%)	Cirrhotic (%)
HCC (explant or resection)	20	1[a], 1[c]	18	100	44
HCC (RFA)	7	0	7	71	100
HCC (TACE)	15	0	15	27	93
Hypervascular metastasis	13	6[a], 1[b]	6	67	17
Regenerative nodule	11	1[b]	10	10	70[d]
FNH	6	2[a]	4	50	0
THAD	10	1[a]	9	0	22
Hemangioma	17	6[a], 4[b]	7	0	0
Adenoma	2	0	2	50	0
Total / Average	101	23	78	45	50

[a] Peak enhancement of the aorta was not during the arterial phase, or peak enhancement of the portal vein was not during the portal venous phase

[b] Enhancing portion of the lesion was too small to characterize (≤5 mm)

[c] Complete occlusion of the main portal vein

[d] Non-cirrhotic cases had Budd-Chiari syndrome

features on MRI (if available). Evaluation for cirrhosis was based on pathology (if available) or based on the CT appearance of the liver.

The study group included 78 liver lesions in 64 patients (Table 1). There were 40 HCCs, 10 regenerative nodules, 9 transient hepatic attenuation differences (THADs) [17], 7 hemangiomas, 6 hypervascular metastases, 4 FNHs, and 2 adenomas. The THADs were secondary to alterations in blood flow from portal vein occlusion (2 cases), hemangioma (1 case), abscess (1 case), around the falciform ligament (1 case), and unknown (4 cases).

Calculation of Hepatic Artery and Portal Vein Blood Supply Coefficients

HAC and PVC were calculated from the pretreatment triphasic CT (arterial, portal venous, and delayed phases). The three phases were manually aligned by translation in the x, y, and z directions. For each phase, regions of interest (ROIs) were drawn over the liver, aorta (at the level of the celiac artery), and portal vein (near the bifurcation). For heterogeneous lesions, measurements were made in the most arterially enhancing portion of the lesion and in the same location on the other phases. ROIs were elliptical, with a length of at least 5 mm. ROIs were also drawn over the background liver. Large intrahepatic vessels were avoided when drawing the ROIs in the liver. The liver enhancement curves were expressed as a linear combination of the hepatic artery and portal venous enhancement curves. Specifically, for each pixel in the liver:

$$x_i = HAC \cdot a_i + PVC \cdot v_i$$

where x_i is the enhancement of the pixel in the liver, a_i is the enhancement of the aorta, and v_i is the enhancement of the portal vein. i=1 is the arterial phase, i=2 is the portal venous phase, and i=3 is the delayed phase. Enhancement was measured in Hounsfield units, relative to the average Hounsfield units of the three phases (we typically do not obtain non-contrast images). Thus,

$$x_i + x_2 + x_3 = 0$$
$$a_1 + a_2 + a_3 = 0$$
$$v_1 + v_2 + v_3 = 0$$

Solving these equations for HAC and PVC yields:

$$\mathrm{HAC} = (v_2x_1 + v_2x_2 + v_3x_2)/(a_2v_3 - a_3v_2)$$
$$\mathrm{PVC} = (a_2x_1 + a_2x_2 + a_3x_2)/(a_3v_2 - a_2v_3)$$

Calculated HAC and PVC for each pixel in the liver were then displayed on both grayscale and color images (Fig. 3 and Appendix). The three color channels in the color image summarize the information from the three post-contrast images. Color images were generated using a custom web application written in PHP, Javascript, and C++.

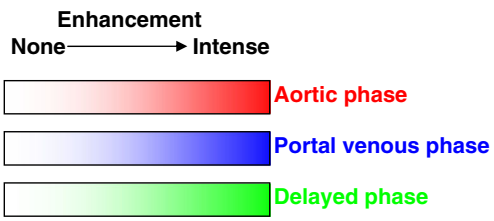

Fig. 3 Color scale for the images in Fig. 6. The *color* indicates the phase of enhancement (based on the HAC and PVC). The *saturation* (grayscale versus color) indicates the degree of enhancement. The *brightness* is related to the average Hounsfield units over the three phases (not shown)

Model Validation

Seven consecutive triphasic liver scans that showed no focal liver lesions and had clearly visualized hepatic veins were evaluated. For each scan, the HAC and PVC of the liver parenchyma were used to calculate the expected enhancement curve of the right hepatic vein:

$$\text{Predicted hepatic vein enhancement} = x_i/(\text{HAC} + \text{PVC})$$

This prediction made by our simple model of liver perfusion was then compared to the measured enhancement.

Lesion Classification and Statistical Analysis

Relative enhancement pattern (density of the most arterially enhancing portion of the lesion compared to the surrounding liver) was based on average Hounsfield unit measurements in the lesion, compared to the surrounding liver, calculated from manually drawn ROIs. Lesions were characterized as hyperdense, isodense, or hypodense relative to surrounding liver in the arterial and delayed phases. For example, "hypervascular with washout" indicates that portions of the lesion are hyperdense relative to the background liver on the arterial phase and those portions become hypodense relative to the surrounding liver on the delayed phase. Lesions were classified as malignant if >y% of lesions with the same relative enhancement pattern were malignant; the sensitivity and specificity of the classification were examined for different values of y [18]. In other words, if a given relative enhancement pattern is always associated with malignant lesions, then that relative enhancement pattern should be considered malignant. If a given relative enhancement pattern is associated with both benign and malignant lesions, then that relative enhancement pattern could be considered either benign or malignant, depending on the value of y, which is adjusted to achieve the desired sensitivity and specificity.

Lesions were also classified as malignant if their HAC and PVC fell within ranges that were similar to other malignant lesions (2D linear classifier). The ranges were chosen to maximize the sum of the sensitivity and specificity [19], using a hill climbing optimization algorithm.

Sensitivity and specificity were calculated on a per-lesion basis. Statistical comparisons were performed using a two-tail, two-sample t test assuming unequal variances. Confidence intervals of proportions were calculated assuming a uniform prior distribution [20]. Differences between proportions were evaluated using a two-tail z-test.

Results

Model Validation

Figure 4 shows good agreement between predicted and measured hepatic vein enhancement. Although predicting hepatic vein enhancement does not have clinical significance, the agreement between the prediction and reality provides some support for our simple model of liver perfusion.

Hepatic Artery and Portal Vein Coefficients

HAC and PVC of non-cirrhotic liver, cirrhotic liver, and various liver lesions are shown in Fig. 5 and Table 2. There was significant overlap between different liver lesions. However, malignant lesions tended to have perfusion characteristics that fell within the gray rectangle, while benign lesions had a wider range of perfusion characteristics and mostly fell outside the gray rectangle. Classification of liver lesions on the basis of perfusion characteristics is described in the next section.

Cirrhotic liver had decreased portal vein coefficient (PVC) compared to normal liver ($p=2.4\times10^{-8}$). HCC had increased hepatic artery coefficient (HAC) compared to the background liver ($p=8.8\times10^{-17}$). Hypervascular metastases had similar HAC and PVC compared to HCCs. Hemangioma had increased HAC compared to HCC.

FNH and THAD both had increased PVC compared to HCC. Two of the THADs were caused by occlusion of a

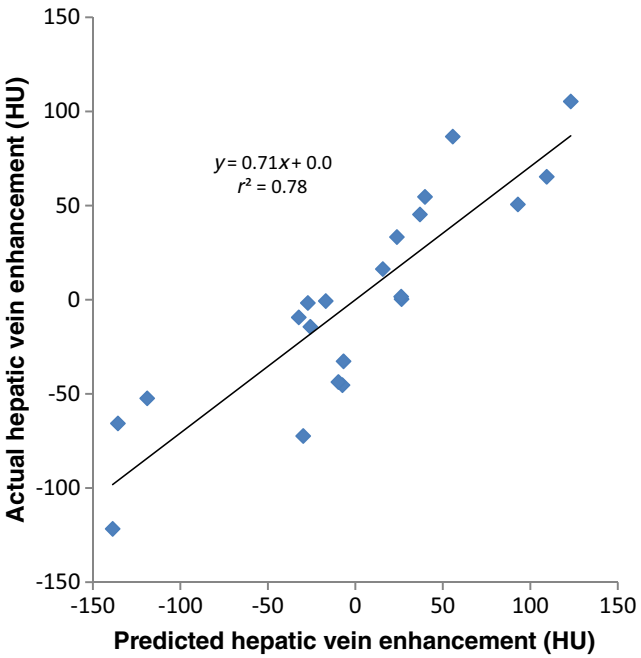

Fig. 4 Predicted versus measured enhancement of the right hepatic vein (Hounsfield units, relative to the average of the three phases). Each point represents a single phase of a single triphasic CT. The predicted enhancement of the hepatic vein is based on the enhancement of the aorta, portal vein, and liver parenchyma

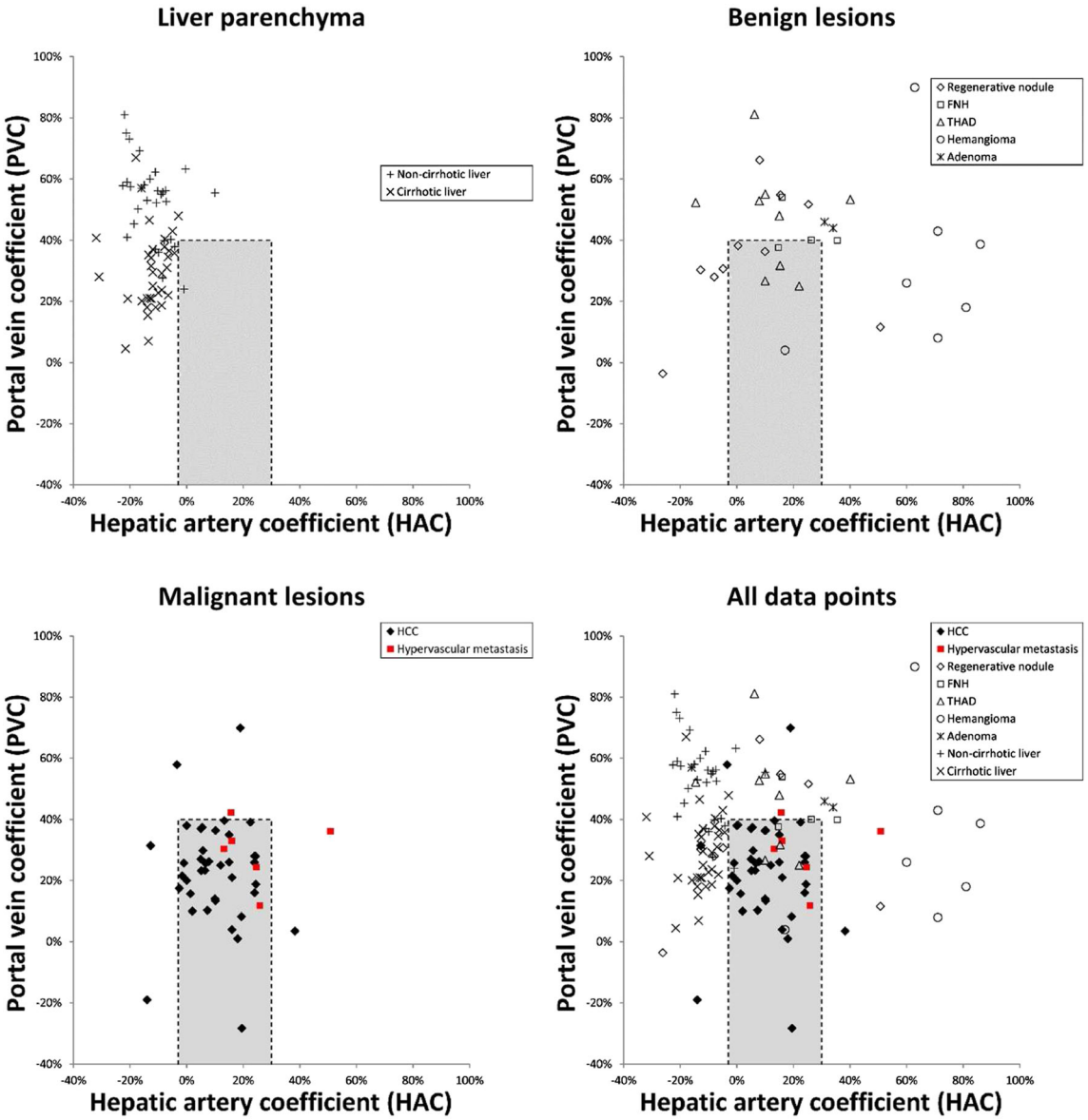

Fig. 5 Hepatic artery and portal vein coefficients for untreated liver lesions, coded by diagnosis. Malignant lesions are shown as *solid filled shapes*, and benign lesions are shown as *open shapes*. Lesions in the *gray rectangle* were classified as malignant. The size and position of the *gray rectangle* were chosen to maximize the sum of the sensitivity and specificity of the classification

branch of the portal vein. In both cases, both the HAC and PVC were increased compared to portions of the liver supplied by a patent portal vein.

Regenerative nodules had a wide range of HAC and PVC, but the average coefficients were not statistically significantly different from HCC. Some regenerative nodules had increased PVC compared to HCC, like THADs. Others had characteristics that overlapped with cirrhotic liver. One nodule had increased HAC compared to HCC, like a hemangioma.

HAC and PVC can be displayed on grayscale or color images (Figs. 3 and 6). Each type of lesion had a characteristic appearance on color images. Notice that the aorta is bright red and the portal vein is bright blue. Normal liver is light blue, indicating that the enhancement curve follows the portal vein but is not as intense. Hypervascular liver lesions are typically purple, indicating that the shape of the enhancement curve is in between that of the aorta and portal vein. Fat and muscle are gray, indicating minimal enhancement. The artifactual color near edges is due to misalignment among the three phases.

Classification of Liver Lesions

In this diverse set of liver lesions, the most suspicious relative enhancement pattern was hypervascularity with washout (Table 3), which was seen in HCC, hypervascular metastases, and some benign lesions. The second most suspicious relative enhancement pattern was hypodensity on all phases, which was seen in HCC and regenerative nodules (hepatic cysts were

Table 2 Hepatic artery coefficients (HAC) and portal vein coefficients (PVC) for various liver lesions (untreated), in ml/ml (%)

Diagnosis	Number	HAC		PVC	
		Average (%)	Standard deviation (%)	Average (%)	Standard deviation (%)
HCC	40	10	11	23	17
Hypervascular metastasis	6	24	14	30	11
Regenerative nodule	10	6	22	34	20
FNH	4	23	10	43*	7
THAD	9	12	14	47*	18
Hemangioma	7	64*	23	33	29
Adenoma	2	33*	2	45*	1
Non-cirrhotic liver[a]	36	−12	7	52	14
Cirrhotic liver[a]	38	−13	7	31	14

*Statistically significant difference compared to HCC. To correct for multiple comparisons, a cutoff p value of 0.05/12=0.0042 was used to determine statistical significance

[a] Excluding liver transplants and Budd-Chiari syndrome. If lesions in both the right and left liver were analyzed, then ROIs were drawn in both the right and left lobes of the liver

not included in this study). Using only the most suspicious relative enhancement pattern (hypervascularity with washout) to diagnose malignant lesions resulted in a sensitivity of 72 % and specificity of 81 %. Using the top two most suspicious relative enhancement patterns (hypervascularity with washout or hypodensity on all phases) to diagnose malignancy resulted in a sensitivity of 89 % and specificity of 72 % (the improved sensitivity was statistically significant, but the decreased specificity was not).

Liver lesions were also classified based on the HAC and PVC. As described above, HCC and hypervascular metastases had similar coefficients, while benign lesions had either greater PVCs (FNH or THAD) or greater HACs (hemangioma). We therefore classified a lesion as malignant if the coefficients were similar to other malignant lesions. The optimal ranges for diagnosing malignancy were as follows: HAC>−3 %, HAC<30 %, and PVC<40 % (Fig. 5). The resulting sensitivity was 85 % and specificity was 78 %. This was not statistically significantly different from using hypervascularity with washout to diagnose malignancy.

Requiring that a lesion be suspicious by both relative enhancement criteria (hypervascular with washout or hypodense on all phases) and HAC and PVC criteria to be diagnosed as malignant resulted in a sensitivity of 76 % and a specificity of 97 % (Table 4). This was a statistically significant improvement in specificity for detecting malignant liver lesions (p=0.039), compared to hypervascularity with washout.

Discussion

The clinical promise of CT perfusion imaging of the liver has largely been unfulfilled, for two major reasons: the increased radiation dose and unclear clinical benefit. In our paper, we address both of these issues. We developed a simplified model of tumor blood supply that can be applied to standard triphasic scans, thus reducing the radiation dose relative to traditional perfusion imaging. We then show that blood volumes estimated from triphasic scans improve the specificity for diagnosing malignancy, compared to traditional criteria such as washout. Improved specificity may be especially helpful in non-cirrhotic livers, where imaging findings are currently considered insufficient for diagnosis of HCC, and biopsy is recommended [5, 6]. To our knowledge, this is the first time that liver perfusion parameters have been used to distinguish benign and malignant liver lesions.

HAC and PVC provide an estimate of the blood volumes in liver lesions. The model of liver perfusion used to calculate these coefficients assumes that enhancement of the liver parenchyma is due to enhancement of small branches of the hepatic artery and portal vein, which follow the enhancement of the aorta and main portal vein, respectively. This assumption is reasonable, given that the liver transit time (approximately 10 s [21]) is less than the contrast bolus length (approximately 30 s). Furthermore, the model was validated by using it to predict the enhancement curves of the hepatic veins.

The model captures important aspects of liver physiology. As expected, cirrhosis decreases the PVC, which corresponds to the reduced portal flow associated with cirrhosis. Portal vein occlusion results in increased HAC and PVC in the affected portion of the liver. We can speculate that this is analogous to the compensatory increased cerebral blood volume caused by vasodilation in an acute ischemic stroke [22].

HAC and PVC calculated from pretreatment triphasic CT scans can be used to classify hypervascular liver lesions. HCC and hypervascular metastases, on average, both had increased HACs compared to the background liver, in agreement with

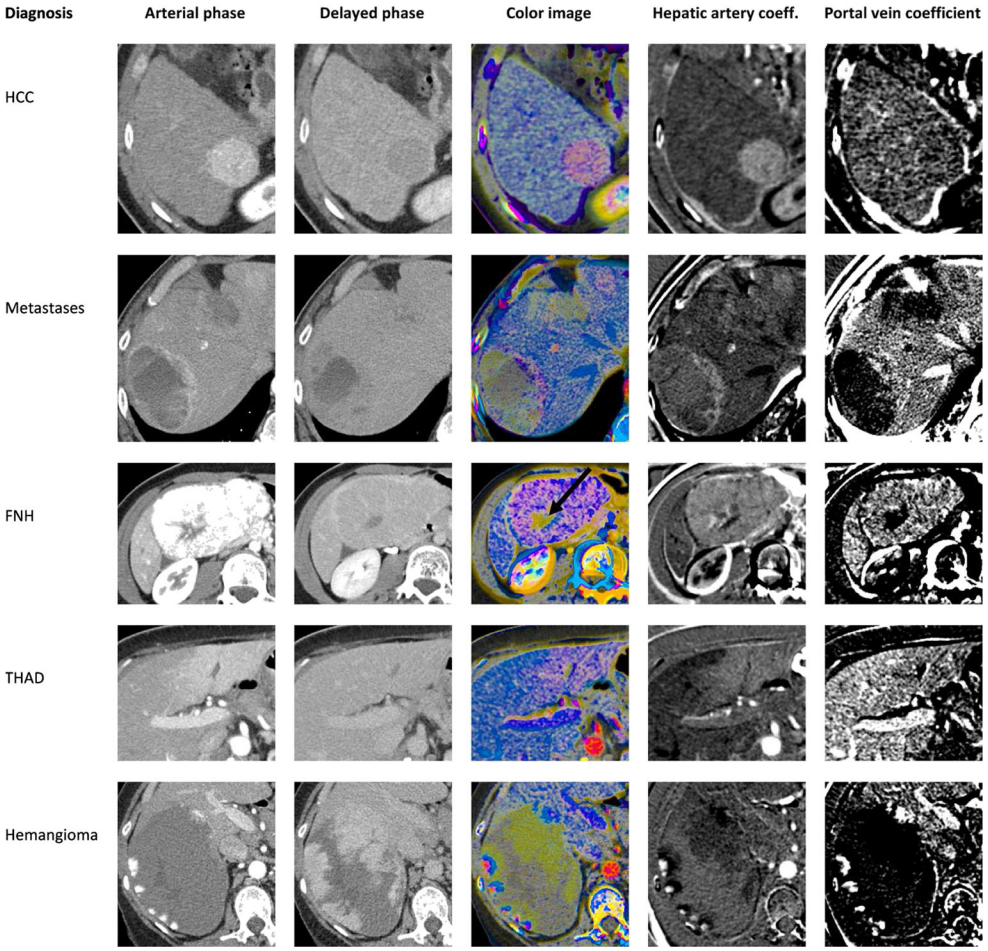

Fig. 6 Hepatic artery and portal vein coefficients, calculated from triphasic scans. The images in each column are displayed at the same window/level settings. The color scale is shown in Fig. 3. The full 3D datasets are available as an interactive figure at http://www.claripacs.com/a.php?a=5q. *Top row* moderately differentiated HCC (pathology proven). The pink color of the lesion indicates predominantly arterial inflow. *Second row* neuroendocrine tumor metastases to the liver (pathology proven). *Third row* focal nodular hyperplasia. Delayed enhancement of the central scar is shown in green (*arrow*) on the color image. The apparent washout of the lesion in the delayed phase is an optical illusion due to the enhancing rim [28]. Hounsfield unit measurements show that the lesion is isodense to the liver on the delayed phase. *Fourth row* THAD surrounding the falciform ligament, which is a common location [17]. *Last row* giant hemangioma. Notice the peripheral foci of arterial phase enhancement (red), with enhancement progressing more centrally on later phases (blue and green)

prior results [15]. Compared to HCC, benign lesions, on average, had either greater PVCs (FNH or THAD) or greater HACs (hemangioma).

The elevated blood volumes in hemangiomas correspond to the increased blood volume seen on tagged red blood cell scans [23].

Table 3 Diagnosis by relative enhancement pattern

Relative enhancement	Number	% Malignant (95 % confidence interval)	Diagnoses
Hypervascular with washout	39	85 (71–94)	HCC (27; 6 well differentiated, 5 moderately differentiated, 1 poorly differentiated, 15 unknown), metastasis (6), hemangioma (3), adenoma (2), and regenerative nodule (1)
Hypervascular on arterial phase and isodense on the delayed phase	18	28 (11–50)	THAD (6), HCC (5; 2 moderately differentiated, 3 unknown), regenerative nodule (3), and FNH (4)
Hypodense on all phases	11	73 (45–92)	HCC (8; 3 well differentiated, 2 moderately differentiated, 3 unknown), and regenerative nodule (3)
Hyperdense on all phases	8	0 (0–28)	Hemangioma (4), THAD (3), and regenerative nodule (1)
Other	2	0 (0–63)	Regenerative nodule (2)

Table 4 Sensitivity and specificity for diagnosing malignant liver lesions (on a per-lesion basis)

Criterion	Sensitivity (%)	Specificity (%)
A. Hypervascular with washout	72	81
B. Hypervascular with washout or hypodense on all phases	89*	72
C. HAC>−3 %, HAC<30 %, and PVC< 40 %	85	78
D. A and C	65	97*
E. B and C	76	97*

Asterisk indicates a statistically significant difference compared to hypervascularity with washout (criterion A)

Regenerative nodules showed three different types of HAC and PVC, which were similar to cirrhotic liver, THADs, and hemangiomas. The clinical significance of these three different classes of coefficients is unclear, but it is possible that some of the lesions that are being diagnosed as "regenerative nodules" based on imaging are actually THADs or hemangiomas.

HAC and PVC improve the specificity for diagnosing malignancy in liver lesions, when combined with traditional relative enhancement criteria (such as washout).

Hypervascularity with washout is a key diagnostic criterion for HCC but had a sensitivity of only 72 % and specificity of 81 % for diagnosing malignancy in a diverse set of liver lesions. Using the HAC and PVC, in addition to the relative enhancement patterns, computer-aided diagnosis resulted in a sensitivity of 76 % and specificity of 97 % for malignancy.

Thus, relative enhancement criteria (such as washout) and HAC and PVC provide complementary information about liver lesions. Washout considers the enhancement of both the lesion as well as the surrounding liver, whereas the HAC and PVC consider only the enhancement of the lesion itself. It

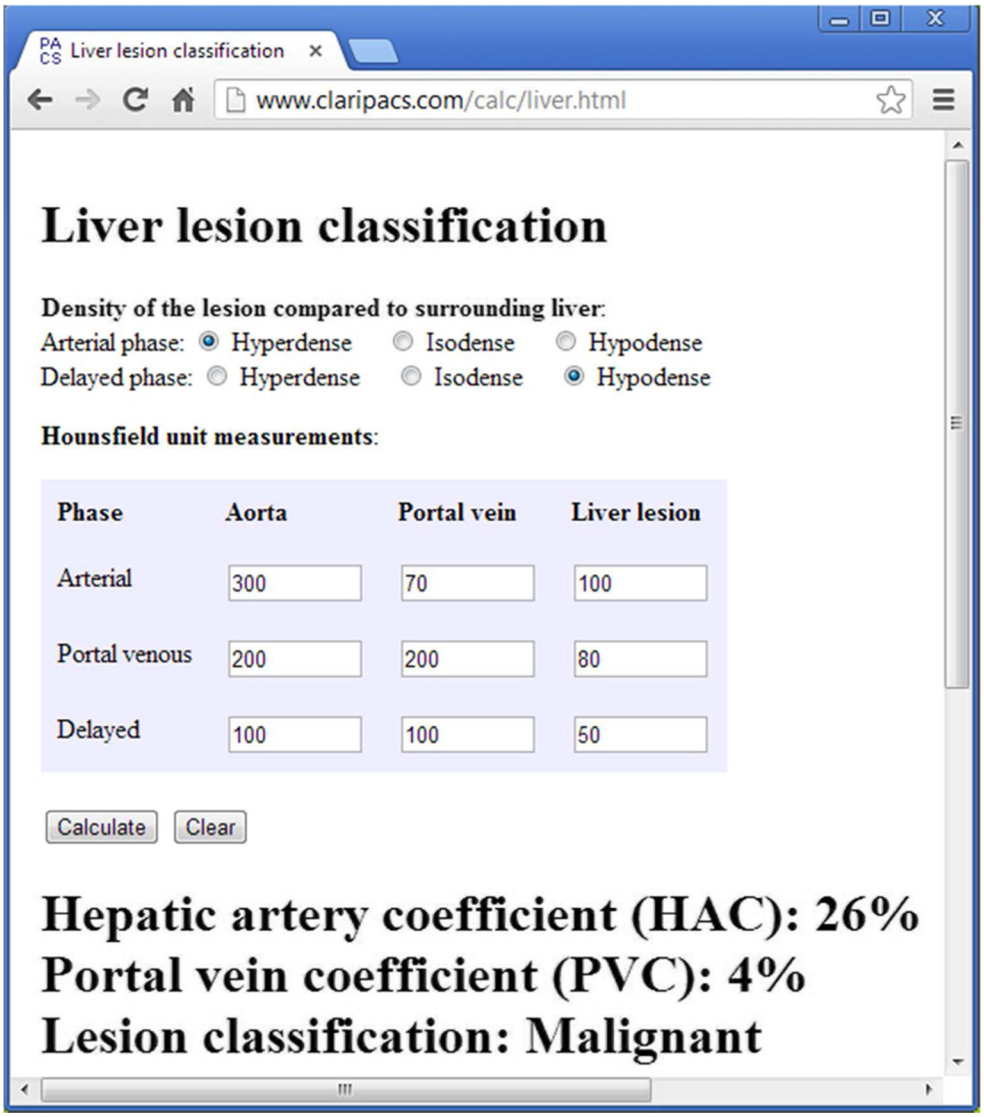

Fig. 7 Online liver lesion classification. See http://www.claripacs.com/calc/liver.html

would be interesting to examine HAC and PVC relative to the surrounding liver, but these would be technically challenging to measure accurately, because subtracting noisy coefficients would double the variance (assuming uncorrelated noise).

We developed an online calculator for liver lesion classification based on relative enhancement, HAC, and PVC: http://www.claripacs.com/calc/liver.html (Fig. 7). Note that this classifier should not be applied to cysts, hypovascular metastases, or cholangiocarcinoma, which were not included in the training set.

The color images in Fig. 6 summarize the information in the three phases of the scan, potentially allowing for a quicker assessment of multiple time points. Each type of liver lesion had a characteristic appearance on the color and grayscale images showing HAC and PVC. These color images encode three numbers per pixel (HAC, PVC, and average Hounsfield units) and thus have a higher information content than prior methods for colorizing multiphasic scans, which encode a single number per pixel [24]. The role of these color images in lesion detection or characterization should be examined in future studies.

There are several limitations to this study. First, the study population was selected to include a diverse set of liver lesions. The frequency of different types of lesions may be different in a different population, which could change the sensitivity, specificity, and pretest probability. For example, the pretest probability of HCC is higher in a cirrhotic liver (resulting in the recommendation that imaging alone can only be used to diagnose HCC in cirrhotic livers [5]). In this paper, we included both cirrhotic and non-cirrhotic livers. Second, we only examined lesion characterization, and not lesion detection, which will result in an overestimation of the sensitivity.

A third limitation is that we only examined HAC, PVC, and relative enhancement characteristics. Several other imaging features can be used to distinguish HCC from other liver lesions: portal vein invasion, abnormal internal vessels [3, 25], heterogeneous enhancement [3], large size [7], hyperintensity on T2 MRI sequences, and a pseudocapsule with delayed enhancement [26] all favor a diagnosis of HCC. Our findings should be confirmed with a prospective study, where the HAC and PVC are considered in the context of all of the other imaging and clinical data.

A fourth limitation is that the HAC and PVC are only equal to the hepatic artery and portal vein blood volumes if there is rapid blood flow and no leakage of contrast from the vessel. These assumptions are not valid when there is delayed enhancement. Delayed enhancement results in calculated blood volumes less than zero, which are not physiologic. Accurate blood volumes are difficult to obtain from the limited information in a triphasic scan. However, our estimated blood volumes were useful for classifying liver lesions, even if they do not quantitatively match the actual blood volumes. A more sophisticated model would require more contrast phases and likely a higher radiation dose. However, a previous study showed that even with 60 time points, the enhancement curves only had sufficient information to fit a three-parameter model, and a five-parameter model was underdetermined [27]. In this paper, we had 3 time points and used a two-parameter model (HVC and PVC). Given the limited information in the enhancement curves, liver perfusion models all make a variety of different assumptions and do not quantitatively match experimental measurements [16, 27].

Finally, the liver deforms with breathing, making it difficult to align exactly across phases. We aligned the phases using translation in three dimensions, but more sophisticated non-rigid alignment algorithms are available [24]. Furthermore, in heterogeneous lesions, we measured the most arterially enhancing portion of the lesion, but the exact choice of ROI is still somewhat arbitrary. Both of these factors introduce uncertainty into the calculated coefficients.

Conclusion

HAC and PVC calculated from triphasic liver CT examinations can be used to classify hypervascular liver lesions. These coefficients improve the specificity for diagnosing malignancy in liver lesions, when combined with traditional relative enhancement criteria (such as washout).

Funding None.

Disclosures None.

Appendix

The red, green, and blue values for each pixel in the color images (ranging from 0 to 1) were calculated from the HAC, PVC, and Hounsfield units (averaged over the arterial, portal venous, and delayed phases), using the following pseudocode. The result is the color scale shown in Fig. 3.

```
// the square root(sqrt) was added empirically to reduce color saturation.
// force_range(x,a,b) equals a if x<a, b if x>b, and x otherwise.
red=sqrt(force_range(1+HAC-PVC, 0, 2));
blue=sqrt(force_range(1-HAC+PVC, 0, 2));
green=sqrt(force_range(1-HAC-PVC, 0, 2));
// scale is used to make the brightness related to the Hounsfield units
if (max(red,green,blue) == 0)
scale=0;
else
scale=force_range((HU-window_level+window_width/2)/window_width, 0, 1)/max(red,green,blue);
red=force_range(red*scale, 0, 1);
blue=force_range(blue*scale, 0, 1);
green=force_range(green*scale, 0, 1);
```

References

1. Iannaccone R, et al: Hepatocellular carcinoma: role of unenhanced and delayed phase multi-detector row helical CT in patients with cirrhosis. Radiology 234:460–467, 2005
2. Doyle DJ, O'Malley ME, Jang HJ, Jhaveri K: Value of the unenhanced phase for detection of hepatocellular carcinomas 3 cm or less when performing multiphase computed tomography in patients with cirrhosis. J Comput Assist Tomogr 31: 86–92, 2007
3. Lee KH, O'Malley ME, Haider MA, Hanbidge A: Triple-phase MDCT of hepatocellular carcinoma. AJR Am J Roentgenol 182: 643–649, 2004
4. Liu YI, Shin LK, Jeffrey RB, Kamaya A: Quantitatively defining washout in hepatocellular carcinoma. AJR Am J Roentgenol 200:84–89, 2013
5. Llovet JM, Ducreux M: EASL-EORTC clinical practice guidelines: management of hepatocellular carcinoma. J Hepatol 56:908–943, 2012
6. Bruix J, Sherman M: Management of hepatocellular carcinoma: an update. Hepatology 53:1020–1022, 2011
7. Bolondi L, et al: Characterization of small nodules in cirrhosis by assessment of vascularity: the problem of hypovascular hepatocellular carcinoma. Hepatology 42:27–34, 2005
8. Kim SH, et al: Gadoxetic acid-enhanced MRI versus triple-phase MDCT for the preoperative detection of hepatocellular carcinoma. AJR Am J Roentgenol 192:1675–1681, 2009
9. Brancatelli G, Baron RL, Peterson MS, Marsh W: Helical CT screening for hepatocellular carcinoma in patients with cirrhosis: frequency and causes of false-positive interpretation. AJR Am J Roentgenol 180:1007–1014, 2003
10. Freeny PC, Marks WM: Hepatic hemangioma: dynamic bolus CT. AJR Am J Roentgenol 147:711–719, 1986
11. Carlson SK, Johnson CD, Bender CE, Welch TJ: CT of focal nodular hyperplasia of the liver. AJR Am J Roentgenol 174: 705–712, 2000
12. Ichikawa T, Federle MP, Grazioli L, Nalesnik M: Hepatocellular adenoma: multiphasic CT and histopathologic findings in 25 patients. Radiology 214:861–868, 2000
13. Sica GT, Ji H, Ros PR: CT and MR imaging of hepatic metastases. AJR Am J Roentgenol 174:691–698, 2000
14. Schenk Jr, WG, Mc DJ, Mc DK, Drapanas T: Direct measurement of hepatic blood flow in surgical patients: with related observations on hepatic flow dynamics in experimental animals. Ann Surg 156:463–471, 1962
15. Li JP, et al: Assessment of tumor vascularization with functional computed tomography perfusion imaging in patients with cirrhotic liver disease. Hepatobiliary Pancreat Dis Int 10:43–49, 2011
16. Pandharipande PV, Krinsky GA, Rusinek H, Lee VS: Perfusion imaging of the liver: current challenges and future goals. Radiology 234:661–673, 2005
17. Desser TS: Understanding transient hepatic attenuation differences. Semin Ultrasound CT MR 30:408–417, 2009
18. Obuchowski NA: Receiver operating characteristic curves and their use in radiology. Radiology 229:3–8, 2003
19. Kaivanto K: Maximization of the sum of sensitivity and specificity as a diagnostic cutpoint criterion. J Clin Epidemiol 61: 517–518, 2008
20. Boas FE: Linkage to Gaucher mutations in the Ashkenazi population: effect of drift on decay of linkage disequilibrium and evidence for heterozygote selection. Blood Cells Mol Dis 26:348–359, 2000
21. Pedersen JF, Larsen VA, Bytzer P, Madsen LG, Hamberg O: Hepatic transit time of ultrasound contrast in biopsy characterized liver disease. Acta radiologica 46:557–560, 2005
22. Hoeffner EG, et al: Cerebral perfusion CT: technique and clinical applications. Radiology 231:632–644, 2004
23. Mettler FA, Guiberteau MJ: Essentials of nuclear medicine imaging, 2012
24. Kim KW, et al: Quantitative CT color mapping of the arterial enhancement fraction of the liver to detect hepatocellular carcinoma. Radiology 250:425–434, 2009
25. Nino-Murcia M, Olcott EW, Jeffrey Jr, RB, Lamm RL, Beaulieu CF, Jain KA: Focal liver lesions: pattern-based classification scheme for enhancement at arterial phase CT. Radiology 215:746–751, 2000
26. Khan AS, Hussain HK, Johnson TD, Weadock WJ, Pelletier SJ, Marrero JA: Value of delayed hypointensity and delayed enhancing rim in magnetic resonance imaging diagnosis of small hepatocellular carcinoma in the cirrhotic liver. J Magn Reson Imaging 32:360–366, 2010
27. Materne R, et al: Non-invasive quantification of liver perfusion with dynamic computed tomography and a dual-input one-compartmental model. Clin Sci (Lond) 99:517–525, 2000
28. Stevens J: Brightness inhibition re size of surround. Perception & psychophysics 2:189–192, 1967